The Abdus Salam
International Centre for Theoretical Physics

United Nations
Educational, Scientific and
Cultural Organization

IAEA
International Atomic Energy Agency

1864-15

Ninth Workshop on Non-linear Dynamics and Earthquake Predictions

1 - 13 October 2007

Applications of Data Assimilation Methods in Geodynamics

Alik T. Ismail-Zadeh

Geophysical Institute
University of Karlsruhe
Karlsruhe, Germany
&
International Institute of Earthquake Prediction Theory & Mathematical Geophysics
Moscow, Russia

United Nations Educational Scientific and Cultural Organization
and
International Atomic Energy Agency

THE ABDUS SALAM
INTERNATIONAL CENTRE FOR THEORETICAL PHYSICS

Ninth Workshop
"Non-Linear Dynamics and Earthquake Prediction"
1 October to 13 October 2007

APPLICATIONS OF DATA ASSIMILATION METHODS IN GEODYNAMICS

Alik T. Ismail-Zadeh

Geophysical Institute, University of Karlsruhe,
Hertzsrt. 16, Karlsruhe 76187, Germany.
E-mail: Alik.Ismail-Zadeh@gpi.uka.de

International Institute of Earthquake Prediction Theory and
Mathematical Geophysics, Russian Academy of Sciences,
84/32 Profsoyuznaya ul., Moscow 117997, Russia.

MIRAMARE-TRIESTE
October 2007

Thermal evolution and geometry of the descending lithosphere beneath the SE-Carpathians: An insight from the past

Alik Ismail-Zadeh*

Institut de Physique du Globe de Paris, 4, Pl. Jussieu, Paris 75005, France

Geophysical Institute, Karlsruhe University, Hertzstr. 16, Karlsruhe 76187, Germany

(aiz@ipgp.jussieu.fr; Alik.Ismail-Zadeh@gpi.uka.de)

Gerald Schubert

Department of Earth and Space Sciences & Institute of Geophysics and Planetary Physics, University of California, 3806 Geology Building, 595 Charles Young Drive East, Los Angeles, CA 90095-1567, USA

(schubert@ucla.edu)

Igor Tsepelev, Alexander Korotkii

Institute of Mathematics and Mechanics, Ural Branch, Russian Academy of Sciences, S. Kovalevskoy ul. 16, Yekaterinburg 620219, Russia

(tsepelev@imm.uran.ru; korotkii@imm.uran.ru)

* Corresponding author.

Phone: +33-1-44272418   *Fax:* +33-1-44273894 (in IPGP)

Phone: +49-721-6084610   *Fax:* +49-721-71173 (in GPI/UKA)

ABSTRACT

Mantle heterogeneities imaged by seismic tomography in the SE-Carpathians contain information on the present thermal state of the mantle. We develop a model of the present crustal and mantle temperature beneath the region based on *P*-wave seismic velocity anomalies and constrained by heat flow data. The present model temperatures are assimilated into the geological past using the information on the history of the regional movement in the Early and Middle Miocene. Prominent thermal states of the lithospheric slab descending in the region are restored from its diffuse present state. In Miocene times the slab geometry clearly shows two portions of the sinking body. The northwest-southeast oriented portion of the body is located in the vicinity of the boundary between the East European and Scythian platforms, and this portion of the sinking body may be a relic of cold lithosphere that has traveled eastward. Another portion has a northeast-southwest orientation and is related to the present descending slab. Above a depth of 60 km the slab had a concave thermal shape, confirming the curvature of the Carpathian arc, and a convex surface below that depth. The slab maintained its convex shape until it split into two parts at a depth of about 220 km. We propose that this change in the slab geometry, which is likely to be preserved until the present, can cause stress localization due to the slab bending and subsequent stress release resulting in large mantle earthquakes in the region. Our results also support the hypothesis of dehydration and partial melting of the descending lithosphere as the cause of the reduction in seismic velocities beneath the Transylvanian Basin.

Key words: mantle structure, mantle dynamics, thermal convection, data assimilation, Vrancea, lithospheric slab, subduction

INTRODUCTION

Repeated large intermediate-depth earthquakes in the southeastern (SE-) Carpathians (the Vrancea region) cause destruction in Bucharest, the capital city of Romania, and shake central and eastern European cities several hundred kilometers away from the hypocenters of the events. The earthquake-prone Vrancea region (Fig. 1) is bounded to the north and northeast by the Eastern European platform (EEP), to the east by the Scythian platform (SCP), to the south-east by the Dobrogea orogen (DOB), to the south and south-west by the Moesian platform (MOP), and to the north-west by the Transylvanian basin (TRB). The epicenters of the sub-crustal earthquakes in the Vrancea region are concentrated within a very small seismogenic volume about 70 km $\times$ 30 km in planform and between depths of about 70 and 180 km. Below this depth the seismicity ends suddenly: one seismic event at 220 km depth is an exception (Oncescu and Bonjer, 1997). Vrancea earthquakes occur in response to stresses generated in the descending lithospheric slab at these depths.

The 1940 M_W=7.7 earthquake gave rise to the development of a number of geodynamic models for this region. McKenzie (1972) suggested that this seismicity is associated with a relic slab sinking in the mantle and now overlain by continental crust. The 1977 large earthquake and later the 1986 and 1990 earthquakes again raised questions about the nature of the earthquakes. A seismic gap at depths of 40-70 km beneath Vrancea led to the assumption that the lithospheric slab had already detached from the continental crust (Fuchs et al., 1979). Oncescu (1984) proposed that the intermediate-depth events are generated in a zone that separates the sinking slab from the neighboring immobile part of the lithosphere rather than in the sinking slab itself. Linzer (1996) explained the nearly vertical position of the Vrancea slab as the final rollback stage of a small fragment of oceanic lithosphere. Various types of slab detachment or delamination (e.g., Girbacea and Frisch, 1998; Wortel and Spakman, 2000; Gvirtzman, 2002; Knapp et al., 2005; Sperner et al., 2005) have been proposed to explain the present-day seismic images of the descending slab. Most recently Cloetingh et al. (2004) argue in favor of the complex configuration of the underthrusted lithosphere and its thermo-mechanical age as primary factors in the behavior of the descending slab after continental collision. The origin of the descending lithosphere in the region, i.e., whether the Vrancea slab is oceanic or continental, is still under debate. Pana and Erdmer (1996) and Pana and Morris (1999) argue that because there is no geological evidence of Mesozoic oceanic crust in the eastern Carpathians, the descending lithosphere is likely to be thinned continental or transitional lithosphere.

The Neogene to Late Miocene (ca. 11 Myr) evolution of the Carpathian region is mainly driven by the northeastward and later eastward roll-back or slab retreat (Royden, 1988; Sperner et al., 2001) of a Carpathians embayment, consisting of the last remnants of an oceanic or thinned continental domain attached to the European continent (e.g., Balla, 1987; Csontos et al., 1992). When the European continent started to enter the subduction zone, the buoyancy forces of the thick continental crust exceeded the slab pull forces and convergence stopped after only a short period of continental thrusting (Sperner et al., 2005). Continental convergence in the SE-Carpathians ceased about 11 Ma (Jiricek, 1979; Csontos et al., 1992), and after that the lithospheric slab descended beneath the Vrancea region due to gravity. The hydrostatic buoyancy forces promote the sinking of the slab, but viscous and frictional forces resist the descent. The combination of these forces produces shear stresses at intermediate depths that are high enough to cause earthquakes (Ismail-Zadeh et al., 2000, 2005b).

The principal aim of this paper is to present a quantitative model of the thermal evolution of the descending slab in the SE-Carpathians using a novel approach for assimilation of present crust/mantle temperature and flow in the geological past (Ismail-Zadeh et al., 2007). The model of the present temperature of the crust and upper mantle is estimated from body wave seismic velocity anomalies and heat flux data and is assimilated into Miocene times. We restore mantle thermal structures and analyze them in the context of modern regional geodynamics.

PRESENT TEMPERATURE MODEL

Temperature is a key physical parameter controlling the density and rheology of the Earth’s material and hence crustal and mantle dynamics. Besides direct measurements of temperature in boreholes in the shallow portion of the crust, there are no direct measurements of deep crustal and mantle temperatures, and therefore the temperatures must be estimated indirectly from seismic wave anomalies, geochemical data, and surface heat flow observations.

We develop a model of the present crustal and mantle temperature beneath the SE-Carpathians using the most recent high-resolution seismic tomography image (map of the anomalies of *P*-wave velocities) of the lithosphere and asthenosphere in the region (Martin et al., 2005, 2006). The tomography image shows a high velocity body beneath the Vrancea region and the Moesian platform interpreted as the subducted lithospheric slab (Martin et al., 2006). The seismic tomographic model of the region consists of eight vertical layers of different thickness (15 km up to 70 km) starting from the depth of 35 km and extending down to a depth of 440 km. Each layer is subdivided horizontally into 16×16-km^2 blocks. To restrict numerical errors in our data assimilation we smooth the velocity anomaly data between the blocks and the layers using a spline interpolation.

We follow the methodology by Goes et al. (2000) and Ismail-Zadeh et al. (2005a) for the inference of temperature estimations from seismic wave anomalies and consider the effects of mantle composition, anelasticity, and partial melting on seismic velocities (see *Appendix A*). The temperature in the crust is constrained by measurements of surface heat flux corrected for paleoclimate changes and for the effects of sedimentation (Demetrescu et al., 2001).

Depth slices of the present temperature model are illustrated in Fig. 2. The pattern of resulting mantle temperature anomalies (predicted temperature minus background temperature) is similar to the pattern of observed *P*-wave velocity anomalies (Martin et al., 2006), but not an exact copy because of the nonlinear inversion of the seismic anomalies to temperature. The low temperatures are associated with the high-velocity body beneath the Vrancea region (VRA) and the East European platform (EEP) and are already visible at depths of 50 km. The slab image becomes clear at 70-110 km depth as a NE-SW oriented cold anomaly. With increasing depth (110–200 km depth) the thermal image of the slab broadens in NW–SE direction. The orientation of the cold body changes from NE–SW to N–S below the depth of 200 km. The slab extends down to 280-320 km depth beneath the Vrancea region itself. A cold anomaly beneath the Transylvanian Basin is estimated at depths of 370–440 km. According to Wortel and Spakman (2000) and Martin et al. (2006) this cold material can be interpreted as a remnant of subducted lithosphere detached during the Miocene along the Carpathian Arc and residing within the upper mantle transition zone. High temperatures are predicted beneath the Transylvanian Basin (TRB) at about 70-110 km depth. Two other high temperature regions are found at 110–150 km depth below the Moesian platform (MOP) and deeper than 200 km under the EEP and the Dobrogea orogen (DOB), which might be correlated with the regional lithosphere/ asthenosphere boundary.

DATA ASSIMILATION

Data assimilation in geodynamical models can be defined as the incorporation of geophysical observations at present and initial physical conditions in the past into a dynamic quantitative model to provide time continuity and coupling among the geophysical fields (e.g., temperature, velocity). The basic principle of data assimilation is to consider the initial temperature in the geological past as a control variable and to optimize the initial temperature in order to minimize the discrepancy between the observations and the solution of the dynamic model (e.g., Bunge et al., 2003; Ismail-Zadeh et al., 2003). Once the initial temperature is determined, the thermal evolution of the mantle can be analyzed (e.g., mantle plume evolution, Ismail-Zadeh et al., 2004, 2006).

To assimilate present temperature and mantle flow beneath the SE-Carpathians, we consider a rectangular three-dimensional domain $\Omega = [0, x_1 = l_1] \times [0, x_2 = l_2] \times [0, x_3 = h]$ and solve numerically, backward in time, the momentum, continuity, and regularized heat equations in the Boussinesq approximation within the model domain (Ismail-Zadeh et al., 2007):

$$\nabla P = \mathrm{div}\left[\eta(T)\mathbf{E}(\mathbf{u})\right] + RaT\mathbf{e}\,, \qquad \mathbf{x} \in \Omega\,, \qquad (1)$$

$$\mathrm{div}\,\mathbf{u} = 0\,, \qquad \mathbf{x} \in \Omega\,, \qquad (2)$$

$$\partial T / \partial t + \mathbf{u} \cdot \nabla T = \nabla^2 T - \beta \Lambda(\partial T / \partial t), \qquad t \in [0, \vartheta],\ \mathbf{x} \in \Omega \qquad (3)$$

with appropriate boundary and initial conditions. Here $\mathbf{x}=(x_1, x_2, x_3)$, $\mathbf{u}=(u_1, u_2, u_3)$, t, T, P, and η are the dimensionless Cartesian coordinates, time, velocity, temperature, pressure, and viscosity, respectively; $\mathbf{e} = (0,0,1)$ is the unit vector; $\mathbf{E} = e_{ij}(\mathbf{u}) = \{\partial u_i / \partial x_j + \partial u_j / \partial x_i\}$ is the strain rate tensor; ∇ is the gradient operator; div is the divergence operator; $[t = 0,\ t = \vartheta]$ is the model time interval; $\Lambda(T) = \partial^4 T / \partial x_1^4 + \partial^4 T / \partial x_2^4 + \partial^4 T / \partial x_3^4$, and β is the regularization parameter. The Rayleigh number is defined as $Ra = \alpha g \rho_{ref} \Delta T h^3 \eta_{ref}^{-1} \kappa^{-1}$, where α is the thermal expansivity, g is the acceleration due to gravity, ρ_{ref} and η_{ref} are the reference density and viscosity, respectively; ΔT is the temperature contrast between the lower and upper boundaries of the model domain; and κ is the thermal diffusivity. Length, temperature, and time are normalized by h, ΔT, and $h^2\kappa^{-1}$, respectively. The physical parameters of the fluid (temperature, velocity, pressure, viscosity, and density) are assumed to depend on time and on space coordinates. Parameters used in the modeling are listed in Table 1. We consider a temperature-dependent Newtonian rheology for the crust and mantle, although the mantle rocks exhibit more complex rheological properties:

$$\eta = \eta_{\text{ref}} \exp\left(Q/(T/T_{\text{ref}} + G) - q/(0.5 + G) \right), \tag{4}$$

where Q = [225/ln(r)] – 0.25 ln(r), G =15/ln(r) – 0.5, r =1000 (Busse et al., 1993).

Our ability to reverse mantle flow is limited by our knowledge of past movements in the region, which are well constrained only in some cases. In reality, the Earth's crust and lithospheric mantle are driven by the gravitational pull of dense descending slabs. However, when a numerical model is constructed for a particular region, external lateral forces can influence the regional crustal movements and hence the style of subduction (flat versus steep subduction). Yet in order to make useful predictions that can be tested geologically, a time-dependent numerical model should include the history of surface motions. Since this is not currently achievable in a dynamical way, it is necessary to prescribe surface motions using velocity boundary conditions.

The simulations are performed backward in time for a period of 22 Myr. We assume perfect slip conditions at the vertical and lower boundaries of the model domain. For the first 11 Myr (starting from the present time), when the rates of continental convergence were insignificant (Jiricek, 1979; Csontos et al., 1992), no velocity is imposed at the surface, and the boundary conditions are free slip. We impose the northwestward velocity in the portion of the upper model boundary (Fig. 3a) for the time interval from 11 Myr to 16 Myr and westward velocity in the same portion of the boundary (Fig. 3b) for the interval from 16 Myr to 22 Myr. The velocities are consistent with the direction and rates of the regional convergence in the Early and Middle Miocene (Morley, 1996; Fügenschuh and Schmid, 2005; Sperner, 2005).

The heat flux through the vertical boundaries of the model domain is set to zero. The upper and lower boundaries are assumed to be isothermal surfaces. The present temperature above 440 km depth is derived from the seismic velocity anomalies. We use the adiabatic geotherm for potential temperature 1750 K (Katsura et al., 2004) to define the present temperature below 440 km (where seismic tomography data are not available).

Equations (1)-(4) with the prescribed boundary and initial conditions are solved numerically by the Eulerian spline finite-element and finite-difference methods. The reader is referred to Ismail-Zadeh et al. (2007) for details of the numerical approach to data assimilation. To estimate the accuracy of the results of data assimilation, we employ the temperature and mantle flow restored to the time of 22 Myr ago as the initial condition for a model of the slab evolution forward in time, run the model to the present, and analyze the temperature residual (the difference between the present temperature and that predicted by the forward model). The maximum temperature residual is estimated to be about 40 degrees.

A sensitivity analysis was performed to understand how stable is the numerical solution to small perturbations in input temperature. The present model temperature has been perturbed randomly by 0.5 to 2% and then assimilated to the past. We found a small misfit between the restored temperature related to the randomly disturbed present temperature and that related to the undisturbed present temperature.

WHAT THE PAST TELLS US

We assimilate the present temperature model into Miocene times to restore the prominent thermal features of the lithospheric slab in the SE-Carpathians (Fig. 4). Although there is some evidence that the slab was already partly subducted some 75 Myr ago (e.g., Sandulescu, 1988), the assimilation interval is restricted in this study to the Miocene, because the pre-Miocene evolution of the descending slab, as well as the regional horizontal movements, are poorly known. Incorporation of poor knowledge into the assimilation model could result in incorrect scenarios of mantle and lithosphere dynamics in the region. Therefore, we have avoided assimilation of the data beyond Miocene time.

Early Miocene subduction beneath the Carpathian arc and the subsequent gentle continental collision transported cold and dense lithospheric material into the hotter mantle. The cold (blue to dark green) region seen at depths of 40 km to 220 km (Fig. 4b-d) can be interpreted as the earlier evolutionary stages of the lithospheric slab. The slab is almost invisible at shallow depth in the model of the present temperature (see relevant slices in Fig. 2 and Fig. 4a). Since active subduction of the lithospheric slab in the region ended in Late Miocene time and earlier rates of convergence were low before it, we argue that the cold slab, descending slowly at these depths, has been warmed up, and its thermal shape has faded due to heat diffusion. Thermal conduction in the shallow Earth (where viscosity is high) plays a significant part in heat transfer compared to thermal convection. The deeper we look in the region, the larger are the effects of thermal advection compared to conduction: the lithosphere has moved upwards to the place where it had been in Miocene times. Below 280 km depth the thermal shape of the slab is clearly visible at the slices of the present temperature model (Figs. 2 and 4a), but it is nearly invisible at the slices of the restored temperature model (Fig. 2b-d), because the slab did not reach these depths in Miocene times.

The geometry of the restored slab (based on the 900 K temperature isotherm) clearly shows two parts of the sinking body (Fig. 4, b-d). The NW-SE oriented part of the body is located in the vicinity of the boundary between the EEP and Scythian platform (SCP) and may be a relic of cold lithosphere that has traveled from the east. Another part has a NE-SW orientation and is associated with the present descending slab. The geometry shows that the restored slab is laterally thin compared to the present thick slab at depths below 90 km. This can be explained by the fact that a slab descending into the mantle thickens with depth and develops a sheath of lithospheric material with time (e.g., Ismail-Zadeh et al., 2005b).

An interesting geometrical feature of the restored slab is its curvature beneath the SE-Carpathians. In Miocene times the slab had a concave surface confirming the curvature of the Carpathian arc down to depths of about 60 km. At greater depths the slab changed its shape to that of a convex surface and split into two parts at a depth of about 200 km. Although such a change in slab curvature is visible neither in the model of the present temperature nor in the seismic tomography image most likely because of slab warming and heat diffusion, we suggest that the convex shape of the slab is likely to be preserved at the present time. We argue that this change in the geometry of the descending slab can cause stress localization due to slab bending and subsequent stress release resulting in earthquakes, which occur at depths of 70 to 180 km in the region. Moreover, the results of the assimilation of the present temperature model to Miocene time provide a plausible explanation for the change in the spatial orientation of the slab from NE-SW to NS beneath 200 km observed in the seismic tomography image (Martin et al., 2006).

The slab bending might be related to a complex interaction between two parts of the sinking body and the surrounding mantle. The sinking body displaces the mantle, which, in its turn, forces the slab to deform due to corner (toroidal) flows different within each of two sub-regions (to NW and to SE from the present descending slab). Also, the curvature of the descending slab can be influenced by slab heterogeneities due to variations in its thickness and viscosity (Cloetingh et al., 2004; Morra et al., 2006).

Martin et al. (2006) interpret the negative velocity anomalies NW of the present slab at depths between 70 and 110 km (see the relevant temperature slices in Figs. 2 and 4a) as a shallow asthenospheric upwelling associated with possible slab rollback. Also, they mention partial melting as an additional contribution to the reduction of seismic velocities at these depths. The results of our assimilation show that the descending slab is surrounded by a narrow border of hotter rocks at depths of 70 to 110 km (the temperature difference between the slab and its surroundings is up to 500 K). Although we do not consider the effects of slab dehydration or partial melting in the modeling, the numerical results obtained support the hypothesis of dehydration of the descending lithosphere and its partial melting as the primary source of reduction of seismic velocities at these depths and probably deeper (see temperature slices at the depths of 130 to 220 km). Some areas of high temperature at depths below 280 km can be associated with mantle upwelling in the region. High-temperature anomalies are not clearly visible in the restored temperatures at these depths, because the upwelling was likely not active in Miocene times.

DISCUSSION AND CONCLUSION

Several processes contribute to the stress generation and its release in the Vrancea region. Among the processes are buoyancy, viscous and frictional forces (Ismail-Zadeh et al., 2000; 2005a,b), plastic instability at high temperature (Griggs and Baker, 1969), faulting due to metamorphic phase transitions (Green and Burnley, 1989; Ismail-Zadeh et al., 2000), and dehydration-induced embrittlement (Ismail-Zadeh et al., 2000; Hacker et al., 2003). We suggest here that bending forces can contribute to the stress field of the descending lithosphere in the SE-Carpathians. The images of the restored earlier stages of the thermal evolution of the mantle in the region show that the descending lithospheric slab changes its curvature from a concave to convex shape, and the area of the maximum bending coincides with the area of intermediate depth Vrancea earthquakes. A concentration of earthquakes associated with slab bending is also seen in other subduction zones, most prominently at the Fiji end of the Tonga slab (Chen and Brudzinskii, 2001).

The negative seismic velocity anomalies and high temperatures beneath the TRB are likely associated with the processes of dehydration and partial melting of wet rocks in the descending lithosphere, rather than with slab rollback and asthenospheric upwelling. An analysis of high-resolution seismic wave attenuation and P- and S-wave seismic tomography images combined with mineral physics can provide estimates of water and melt contents in the region.

Using data assimilation we have shown that the geometry of the mantle structures changes with time, diminishing the degree of surface curvature of the structures. Like Ricci flow, which tends to diffuse regions of high curvature into ones of lower curvature (Hamilton, 1982; Perelman, 2002), heat conduction smooths the complex thermal surfaces of mantle bodies. Present seismic tomography images of mantle structures do not allow definition of the sharp shapes of these structures. Assimilation of mantle temperature and flow to the geological past instead provides a quantitative tool to restore thermal shapes of prominent structures in the past from their diffusive shapes at present.

There are at least two sources of error in data assimilation (apart from the errors associated with the numerical modeling): data misfit related to the uncertainties in the present temperature distribution and/or in the surface movements and errors due to the uncertainties in initial and boundary conditions.

Many models of mantle temperature are based on the conversion of seismic tomography data. The key to an appropriate interpretation of seismic velocity anomalies in tomographic studies is a detailed resolution analysis. Martin et al. (2006) studied the theoretical resolution of their tomography model for the SE-Carpathians by analyzing the resolving width (RW) functional. The RW functional presents the quality of the resolution for the velocity at predefined nodes: its values decrease for well-resolved nodes and increase with the amount of smearing. Figure 2 presents the areas, bounded by the white contour lines, where the values of the RW functional do not exceed 4.0 (compared to 2.0 in the best case and 8.0 in the worth case of the tomography resolution). Therefore, the results of temperature conversion from the seismic tomography model of Martin et al. (2006) should be reliable, at least in the areas of high tomography resolution.

Other sources of uncertainty in the modeling of mantle temperature come from the choice of mantle composition, the seismic attenuation model, and poor knowledge of the presence of water at mantle depths. There are no available data on the composition of the mantle beneath the SE-Carpathians, except a few petrological studies of igneous rocks from the Neogene eastern Carpathian volcanic zone (Nitoi et al., 2002). The drop of electrical resistivity below 1 Ω m (Stanica and Stanica, 1993) can be an indicator of the presence of fluids (due to dehydration of mantle rocks) below the SE-Carpathians; however, the information is very limited and cannot be used in quantitative modeling. Therefore, if the present mantle temperature model is biased, the information can be improperly propagated to the geological past.

The conditions at the boundaries of the model domain used in the data assimilation are, of course, an approximation to the real temperature, heat flux, and movements, which are practically unknown and, what is more important, may change over time at these boundaries. The results of data assimilation will hence depend on the model boundary conditions. Moreover, errors associated with the knowledge of the temperature (or heat flux) evolution or of the regional horizontal surface movements can propagate into the past during data assimilation.

Though interpretation of seismic tomography in terms of temperature and temperature assimilation are somewhat uncertain, we believe that data assimilation is useful for improving our understanding of the thermal and dynamic evolution of the Earth’s crust and mantle. New high-resolution experiments on seismic wave attenuation, improved knowledge of crustal and mantle mineral composition, accurate GPS measurements of regional movements, and precise geological paleoreconstructions of crustal movements in the SE-Carpathians will help refine the present model and our knowledge of the regional thermal evolution.

ACKNOWLEDGMENTS

The authors are very grateful to S. Cloetingh, S. Honda, D. Pana, and S. Sobolev for discussions and constructive comments on the initial version of this paper and to M. Martin and F. Wenzel for the seismic tomography data of the Vrancea region made available for the research. This work was supported by the French-Russian Collaboration Program, the German Research Foundation, and the Russian Academy of Sciences.

APPENDIX A: INVERSION OF *P*-WAVE SEISMIC VELOCITY ANOMALIES INTO TEMPERATURE

Non-linear teleseismic body wave tomography with data of the 1999 Carpathian Arc Lithosphere X-Tomography experiment in Romania provides high-resolution imaging of the upper-mantle structure (Martin et al., 2006). 194 teleseismic events are used for the seismic tomography study in the SE-Carpathians. All data were recorded at the 110 seismic stations (including 24 broad-band stations with a sampling rate ≥50 Hz in the field), which were located densely around the Vrancea region. All seismograms were bandpass filtered between 0.5–2 Hz to enhance the suitable phases *P* and *PKP*, and all earthquake hypocenters were taken from the relocated earthquake catalogue of Engdahl et al. (1998). Source effects and path effects between source and model are effectively removed in teleseismic tomography by using weighted relative residuals for each event (e.g., Evans and Achauer, 1993). Smearing from strong crustal velocity anomalies into the upper mantle was suppressed by travel-time corrections with a priori three-dimensional regional crustal velocity model (Martin et al., 2005). Travel-time residuals were calculated relative to the IASP91 earth model (Kennett and Engdahl, 1991).

The seismic velocity anomalies in the upper mantle can be attributed to variations in temperature (Forte et al., 1994, 1995), although several factors other than temperature can also exert an influence on seismic velocity, e.g., composition (Griffin et al., 1998), anelasticity (Karato, 1993), and presence of melt or water (Karato, 2004). Therefore, in the forward modeling of synthetic *P*-wave seismic velocity anomalies beneath the SE-Carpathians we consider the effects of anharmonicity (composition), anelasticity and partial melting on seismic velocities.

The anharmonic (frequency independent and non-attenuating) part of the synthetic velocities is calculated on the basis of published data on laboratory measurements of density and elastic parameters of the main rock-forming minerals (Bass, 1995) at various thermodynamic conditions. We accept the following model of a composite mineralogy: 57.9% Ol, 16.3% CPx, 13.5% Opx, and 12.3% Gt for the crust and mantle (Green and Falloon, 1998) and 69% Ol, 10% CPx, 19% Opx, and 2% Gt for the slab (Agee, 1993). For each single mineral constituting the models of crust/mantle composition density ρ, thermal expansivity α, the elastic bulk modulus K and shear modulus μ and their pressure and temperature derivatives should be estimated at ambient condition (T_0, P_0) to determine the anharmonic part of the velocity V_{anh} depending on temperature T and pressure P (Goes et al., 2000).

Viscoelastic relaxation at high temperature leads to frequency dependence of seismic wave velocities and attenuation of seismic waves (e.g., Kanamori and Anderson, 1977; Karato, 1993). Shear anelasticity in minerals at high temperatures and low frequencies can be represented by the following relationship: $Q_\mu(\omega, P, T) = B\omega^a \exp\left(\frac{aH}{RT}\right)$, where the Q-factor is defined as the ratio of elastic energy stored in a system to the energy loss per unit cycle, B (=0.148) is a normalization factor, ω (=1 Hz) is the frequency, a (=0.15) is the exponent describing the frequency dependence of the attenuation, H ($= 5\times10^5$ J mol^{-1}) is the activation enthalpy, and R is the universal gas constant. The values for B, a, and H are based on various experimental data (e.g., Karato, 2004). The frequency is consistent with the seismic frequency of PREM (Dziewonski and Anderson, 1981) and AK135 (Montagner and Kennett, 1996). Therefore, the synthetic velocity V_{syn} accounting for the anelasticity can be calculated as

$$V_{syn}(P,T) = V_{anh}(P,T)\left[1 - \frac{Q^{-1}(\omega,P,T)}{2\tan\left(\pi a/2\right)}\right],$$

where $Q^{-1} = (1-L)Q_K^{-1} + LQ_\mu^{-1}$, $L = 4V_S^2 \big/ 3V_P^2$, and Q_K = 57822 (Dziewonski and Anderson, 1981). Once the synthetic velocities are calculated for a first-guess temperature, an iteration process is used to find the temperature $T^n = T_{bg} + \delta T^n$, minimizing the difference between the synthetic $\delta V_{syn} = \left(V_{syn}(P,T_{bg}) - V_{syn}(P,T)\right) \big/ V_{syn}(P,T_{bg})$ and 'observed' δV_{obs} (in seismic tomography experiments) velocity anomalies:

$$\delta T^{n+1} = \delta T^n + F_d\left(\delta V_{obs} - \delta V_{syn}\right) \Big/ \frac{\partial V_{syn}}{\partial T} \to \min_T \quad \text{at} \quad T < T_{sol},$$

$$\delta T^{n+1} = \delta T^n + F_d\left(\delta V_{obs} - \delta V_{syn} - \frac{\partial V_{syn}}{\partial \delta m}\delta m\right) \Big/ \frac{\partial V_{syn}}{\partial T} \to \min_T \quad \text{at} \quad T > T_{sol},$$

where $F_{damp} = \frac{\pi a/2}{\tan(\pi a/2)}$ is the damping factor. The values $\frac{\partial V_{syn}}{\partial \delta m}$ are obtained experimentally (Sato et al., 1989), and δm is the degree of partial melting obtained from McKenzie and Bickle (1988). We used the solidus temperature T_{sol} of a dry peridotite

(Takahashi, 1986). The laterally averaged temperature in the crust and mantle modeled by Demetrescu and Andreescu (1994) was chosen as the background temperature T_{bg} for the inversion of seismic velocity anomalies to temperature (see Fig. 3, Ismail-Zadeh et al., 2005a). The temperature in the shallow levels of the region is constrained from measured surface heat flux corrected for paleoclimate changes and for the effects of sedimentation (Demetrescu et al., 2001).

We note that the model of the present temperature by Ismail-Zadeh et al. (2005a) is based on the previous seismic-tomographic model of Martin et al. (2003), where the variations in crustal thickness were not considered in travel time calculations. The seismic-tomographic model by Martin et al. (2006) is now used to convert the seismic velocity anomalies beneath the region into temperature.

REFERENCES

Agee, C.B., 1993. Petrology of the mantle transition zone. Ann. Rev. Earth Planet. Sci. 21, 19–41.

Balla, Z., 1987. Tertiary paleomagnetic data for the Carpatho-Pannonian region in the light of Miocene rotation kinematics. Tectonophysics 139, 67–98.

Bass, J.D., 1995. Elasticity of minerals, glasses, and melts, in: Ahrens, T.J. (Ed.), Mineral Physics and Crystallography, A Handbook of Physical Constants. Amer. Geophys. Union, Washington, D.C., pp. 45–63.

Bunge, H.-P, Hagelberg, C.R., Travis, B.J., 2003. Mantle circulation models with variational data assimilation: Inferring past mantle flow and structure from plate motion histories and seismic tomography. Geophys. J. Int. 152, 280–301.

Busse, F.H., Christensen, U., Clever, R., Cserepes, L., Gable, C., Giannandrea, E., Guillou, L., Houseman, G., Nataf, H.-C., Ogawa, M., Parmentier, M., Sotin, C., Travis, B., 1993. 3D convection at infinite Prandtl number in Cartesian geometry – a benchmark comparison. Geophys. Astrophys. Fluid Dyn. 75, 39–59.

Chen, W.-P., Brudzinski, M.R., 2001. Evidence for a large-scale remnant of subducted lithosphere beneath Fiji. Science 292, 2475–2479.

Cloetingh, S.A.P.L., Burov, E., Matenco, L., Toussaint, G., Bertotti, G., Andriessen, P.A.M., Wortel, M.J.R., Spakman, W., 2004. Thermo-mechanical controls on the model of continental collision in the SE Carpathians (Romania), Earth Planet. Sci. Lett. 218, 57–76.

Csontos, L., Nagymarosy, A., Horvath, F., Kovac, M., 1992. Tertiary evolution of the intra-Carpathian area; a model. Tectonophysics 208, 221–241.

Demetrescu, C., Andreescu, M., 1994. On the thermal regime of some tectonic units in a continental collision environment in Romania. Tectonophysics 230, 265–276.

Demetrescu, C., Nielsen, S.B., Ene, M., Serban, D.Z., Polonic, G., Andreescu, M., Pop, A., Balling, N., 2001. Lithosphere thermal structure and evolution of the Transylvanian Depression – insight from new geothermal measurements and modelling results. Phys. Earth Planet. Inter. 126, 249–267.

Dziewonski, A.M., Anderson, D.L., 1981. Preliminary Reference Earth Model (PREM): Phys. Earth Planet. Inter. 25, 297–356.

Engdahl, E.R., van der Hilst, R., Buland, R., 1998. Global teleseismic earthquake relocation with improved travel times and procedure for depth determination. Bull. Seism. Soc. Am. 88, 722–743.

Evans, J.R., Achauer, U., 1993. Teleseismic velocity tomography using the ACH-method: theory and application to continental-scale studies, in: Iyer, K.M. Hirahara, K. (Eds.), Seismic Tomography: Theory and Practise, Chapman & Hall, London, pp. 319–360.

Forte, A.M., Dziewonski, A.M., O'Connell, R.J., 1995. Thermal and chemical heterogeneity in the mantle: A seismic and geodynamic study of continental roots. Phys. Earth Planet. Inter. 92, 45–55.

Forte, A.M., Woodward, R.L., Dziewonski, A.M., 1994. Joint inversions of seismic and geodynamic data for models of three-dimensional mantle heterogeneity. J. Geophys. Res. 99, 21857–21887.

Fuchs, K., Bonjer, K., Bock, G., Cornea, I., Radu, C., Enescu, D., Jianu, D., Nourescu, A., Merkler, G., Moldoveanu, T., Tudorache, G., 1979. The Romanian earthquake of March 4, 1977. II. Aftershocks and migration of seismic activity. Tectonophysics 53, 225–247.

Fügenschuh, B., Schmid, S.M., 2005. Age and significance of core complex formation in a very curved orogen: Evidence from fission track studies in the South Carpathians (Romania). Tectonophysics 404, 33–53.

Girbacea, R., Frisch, W., 1998. Slab in the wrong place: Lower lithospheric mantle delamination in the last stage of the Eastern Carpathian subduction retreat. Geology 26, 611–614.

Goes, S., Govers, R., Vacher, P., 2000. Shallow mantle temperatures under Europe from P and S wave tomography. J. Geophys. Res. 105, 11153–11169.

Green, D.H., Falloon, T.J., 1998. Pyrolite: A Ringwood concept and its current expression, in: Jackson, I. (Ed.), The Earth's Mantle. Cambridge University Press, Cambridge, pp. 311–378.

Green, H. W. II, Burnley, P. C., 1989. A new self-organizing mechanism for deep-focus earthquakes. Nature 341, 733–737.

Griffin, W.L., O'Reilly, S.Y., Ryan, C.G., Gaul, O., Ionov, D.A., 1998. Secular variation in the composition of subcontinental lithospheric mantle: Geophysical and geodynamic implications, in: Braun, J. et al. (Eds.), Structure and Evolution of the Australian Continent, Amer. Geophys. Union, Geodyn. Ser., 26, Washington, D.C., pp. 1-26.

Griggs, D. T., Baker, D. W., 1969. The origin of deep-focus earthquakes, in: Mark, H., Fernbach, S. (Eds.), Properties of Matter Under Unusual Conditions, Wiley, New York, pp. 23–42.

Gvirtzman, Z., 2002. Partial detachment of a lithospheric root under the southeast Carpathians: toward a better definition of the detachment concept. Geology 30, 51– 54.

Hacker, B. R., Peacock, S. M., Abers, G. A., Holloway, S. D., 2003. Subduction factory. 2. Are intermediate-depth earthquakes in subducting slabs linked to metamorphic dehydration reactions? J. Geophys. Res. 108, doi:10.1029/ 2001JB001129.

Hamilton, R.S., 1982. Three manifolds with positive Ricci curvature. J. Diff. Geom. 17, 255–306.

Ismail-Zadeh, A.T., Korotkii, A. I., Tsepelev, I.A., 2003. Numerical approach to solving problems of slow viscous flow backwards in time, in: Bathe, K.J. (Ed.), Computational Fluid and Solid Mechanics, Elsevier Science, Amsterdam, pp. 938–941.

Ismail-Zadeh, A., Mueller, B., Schubert, G., 2005a Three-dimensional modeling of present-day tectonic stress beneath the earthquake-prone southeastern Carpathians based on integrated analysis of seismic, heat flow, and gravity observations. Phys. Earth Planet. Inter. 149, 81–98.

Ismail-Zadeh, A., Mueller, B., Wenzel, F., 2005b. Modelling of descending slab evolution beneath the SE-Carpathians: Implications for seismicity, in: Wenzel, F. (Ed.), Perspectives in Modern Seismology, Lecture Notes in Earth Sciences, Volume 105, Springer-Verlag, Heidelberg, pp. 205–226.

Ismail-Zadeh, A.T., Panza, G.F., Naimark, B.M., 2000. Stress in the descending relic slab beneath the Vrancea region, Romania. Pure Appl. Geophys. 157, 111–130.

Ismail-Zadeh, A., Korotkii, A., Schubert, G., Tsepelev, I., 2007. Quasi-reversibility method for data assimilation in models of mantle dynamics. Geophys. J. Int., in press.

Ismail-Zadeh, A, Schubert, G., Tsepelev, I. Korotkii, A., 2004. Inverse problem of thermal convection: Numerical approach and application to mantle plume restoration. Phys. Earth Planet. Inter. 145, 99–114.

Ismail-Zadeh, A., Schubert, G., Tsepelev, I., Korotkii, A., 2006. Three-dimensional forward and backward numerical modeling of mantle plume evolution: Effects of thermal diffusion, J. Geophys. Res. 111, B06401, doi:10.1029/2005JB003782.

Jiricek, R., 1979. Tectonic development of the Carpathian arc in the Oligocene and Neogene, in: Mahel, M. (Ed.), Tectonic Profiles Through the Western Carpathians, Geol. Inst., Dionyz Stur, pp. 205–214.

Kanamori, H., Anderson, D.L., 1977. Importance of physical dispersion in surface-wave and free-oscillation problems – Review. Rev. Geophys. Space Phys. 15, 105–112.

Karato, S.-I., 1993. Importance of anelasticity in the interpretation of seismic tomography. Geophys. Res. Lett. 20, 1623–1626.

Karato, S.-I., 2004. Mapping water content in the upper mantle, in: Eiler, J. (Ed.), Inside the Subduction Factory. Amer. Geophys. Union, Geophys. Monogr. Ser. 138, Washington, D.C., pp. 135–152.

Katsura, T., Yamada, H., Nishikawa, O., Song, M., Kubo, A., Shinmei, T., Yokoshi, S., Aizawa, Y., Yoshino, T., Walter, M.J., Ito, E., Funakoshi, K., 2004. Olivine-wadsleyite transition in the system (Mg, Fe)$_2$SiO$_4$. J. Geophys. Res. 109, B02209, doi:10.1029/2003JB002438.

Kennett, B.L.N., Engdahl, E.R., 1991. Travel times for global earthquake locations and phase identification. Geophys. J. Int. 105, 429–465.

Knapp, J.H., Knapp, C.C., Raileanu, V., Matence, L., Mocanu, V., Dinu, C., 2005. Crustal constraints on the origin of mantle seismicity in the Vrancea Zone, Romania: The case for active continental lithospheric delamination. Tectonophysics 410, 311–323.

Linzer, H.-G., 1996. Kinematics of retreating subduction along the Carpathian arc, Romania. Geology 24, 167–170.

Martin, M., the CALIXTO working group, 2003. High resolution teleseismic P-wave tomography for SE-Romania. Geophys. Res. Abst. 5, 10512.

Martin, M., Ritter, J.R.R., the CALIXTO working group, 2005. High-resolution teleseismic body-wave tomography beneath SE Romania – I. Implications for three-dimensional versus one-dimensional crustal correction strategies with a new crustal velocity model. Geophys. J. Int. 162, 448–460.

Martin, M., Wenzel, F., the CALIXTO working group, 2006. High-resolution teleseismic body wave tomography beneath SE-Romania – II. Imaging of a slab detachment scenario: Geophys. J. Int. 164, 579–595.

McKenzie, D. P., 1972. Active tectonics of the Mediterranean region. Geophys. J. Roy. Astr. Soc. 30, 109–185.

McKenzie, D.P., Bickle, M.J., 1988. The volume and composition of melt generated by extension of the lithosphere. J. Petrol. 29, 625–679.

Montagner, J.-P., Kennett, B.L.N., 1996. How to reconcile body-wave and normal-mode reference Earth models. Geophys. J. Int. 125, 229–248.

Morley, C.K., 1996. Models for relative motion of crustal blocks within the Carpathian region, based on restorations of the outer Carpathian thrust sheets. Tectonics 15, 885–904.

Morra, G., Regenauer-Lieb, K., Giardini, D., 2006. Curvature of oceanic arcs. Geology 34, 877–880.

Nitoi, E., Munteanu, M., Marincea, S., Paraschivoiu, V., 2002. Magma-enclave interactions in the East Carpathian Subvolcanic Zone, Romania: petrogenetic implications. J. Volcan. Geother. Res. 118, 229–259.

Oncescu, M.C., 1984. Deep structure of the Vrancea region, Romania, inferred from simultaneous inversion for hypocentres and 3-D velocity structure. Ann. Geophys. 2, 23–28.

Oncescu, M.C., Bonjer, K.P., 1997. A note on the depth recurrence and strain release of large Vrancea earthquakes. Tectonophysics 272, 291–302.

Pana, D., Erdmer, P., 1996. Kinematics of retreating subduction along the Carpathian arc, Romania: Comment. Geology24, 862–863.

Pana, D., Morris, G.A., 1999. Slab in the wrong place: Lower lithospheric mantle delamination in the last stage of the Eastern Carpathian subduction retreat: Comment. Geology 27, 665–666.

Perelman, G., 2002. The entropy formula for the Ricci flow and its geometric applications, http://arxiv.org/abs/math.DG/0211159.

Royden, L.H., 1988. Late Cenozoic tectonics of the Pannonian basin system, Am. Assoc. Petrol. Geol. Mem. 45, 27–48.

Sandulescu, M., 1988. Cenozoic Tectonic History of the Carpathians, Am. Assoc. Petrol. Geol. Mem. 45, 17–25.

Sato, H., Sacks, I.S., Murase, T., Muncill, G., Fukuyama, H., 1989. QP-melting temperature relation in peridotite at high pressure and temperature: attenuation mechanism and implications for the mechanical properties of the upper mantle. J. Geophys. Res. 94, 10647–10661.

Sperner, B., the CRC 461 Team, 2005. Monitoring of slab detachment in the Carpathians, in: Wenzel, F. (Ed.), Challenges for Earth Sciences in the 21st Century. Springer-Verlag, Heidelberg, pp. 187–202.

Sperner, B., Lorenz, F., Bonjer, K., Hettel, S., Müller, B., Wenzel, F., 2001. Slab break-off – abrupt cut or gradual detachment? New insights from the Vrancea region (SE Carpathians, Romania). Terra Nova 13, 172–179.

Stanica, D., Stanica, M., 1993. An electrical resistivity lithospheric model in the Carpathian orogen from Romania. Phys. Earth Planet. Inter. 81, 99–105.

Takahashi, E., 1986. Melting of a dry peridotite KLB-1 up to 14 GPa: implications on the origin of peridotitic upper mantle. J. Geophys. Res. 91, 9367–9382.

Wortel, M.J.R., Spakman, W., 2000. Subduction and slab detachment in the Mediterranean–Carpathian region. Science 290, 1910–1917.

TABLE 1. Model parameters and values

Parameter	**Symbol**	**Value**
Horizontal dimensions	l_1, l_2 ($l_1 = l_2$)	1005 km
Depth of domain	h	670 km
Acceleration due to gravity	g	9.8 m s^{-2}
Thermal expansivity	α	3×10^{-5} K^{-1}
Thermal diffusivity	κ	10^{-6} m^2 s^{-1}
Reference density	ρ_{ref}	3400 kg m^{-3}
Reference temperature	T_{ref}	2000 K
Surface temperature	T_{surf}	300 K
Temperature drop	$\Delta T = T_{ref} - T_{surf}$	1700 K
Reference viscosity	η_{ref}	10^{21} Pa s
Rayleigh number	Ra	5.2×10^5
Regularization parameter	β	10^{-6}

FIGURE CAPTIONS

Fig. 1. Topography map of the SE-Carpathians and epicenters of Vrancea earthquakes (magnitude ≥ 3). Upper right panel presents hypocenters of the same earthquakes projected onto the NW-SE vertical plane AB. DOB, Dobrogea orogen; EEP, Eastern European platform; MOP, Moesian platform; SCP, Scythian platform; TRB, Transylvanian basin; and VRA, Vrancea.

Fig. 2. Present temperature model as the result of the inversion of the P-wave velocity model. Theoretically well-resolved regions are bounded by dashed line (see text and Martin et al., 2006). Each slice presents a part of the horizontal section of the model domain corresponding to $[x_1 = 177.5 \text{ km}, x_1 = 825.5 \text{ km}] \times [x_2 = 177.5 \text{ km}, x_2 = 825.5 \text{ km}]$, and the isolines present the surface topography (also in Figs. 3 and 4).

Fig. 3. Imposed model surface velocity in data assimilation for the time interval from 11 Myr to 16 Myr (a) and for that from 16 Myr to 22 Myr (b).

Fig. 4. Present temperature (a) and temperatures obtained by the assimilation of the present temperature to the time of 11 Myr (b), 16 Myr (c), and 22 Myr(d).

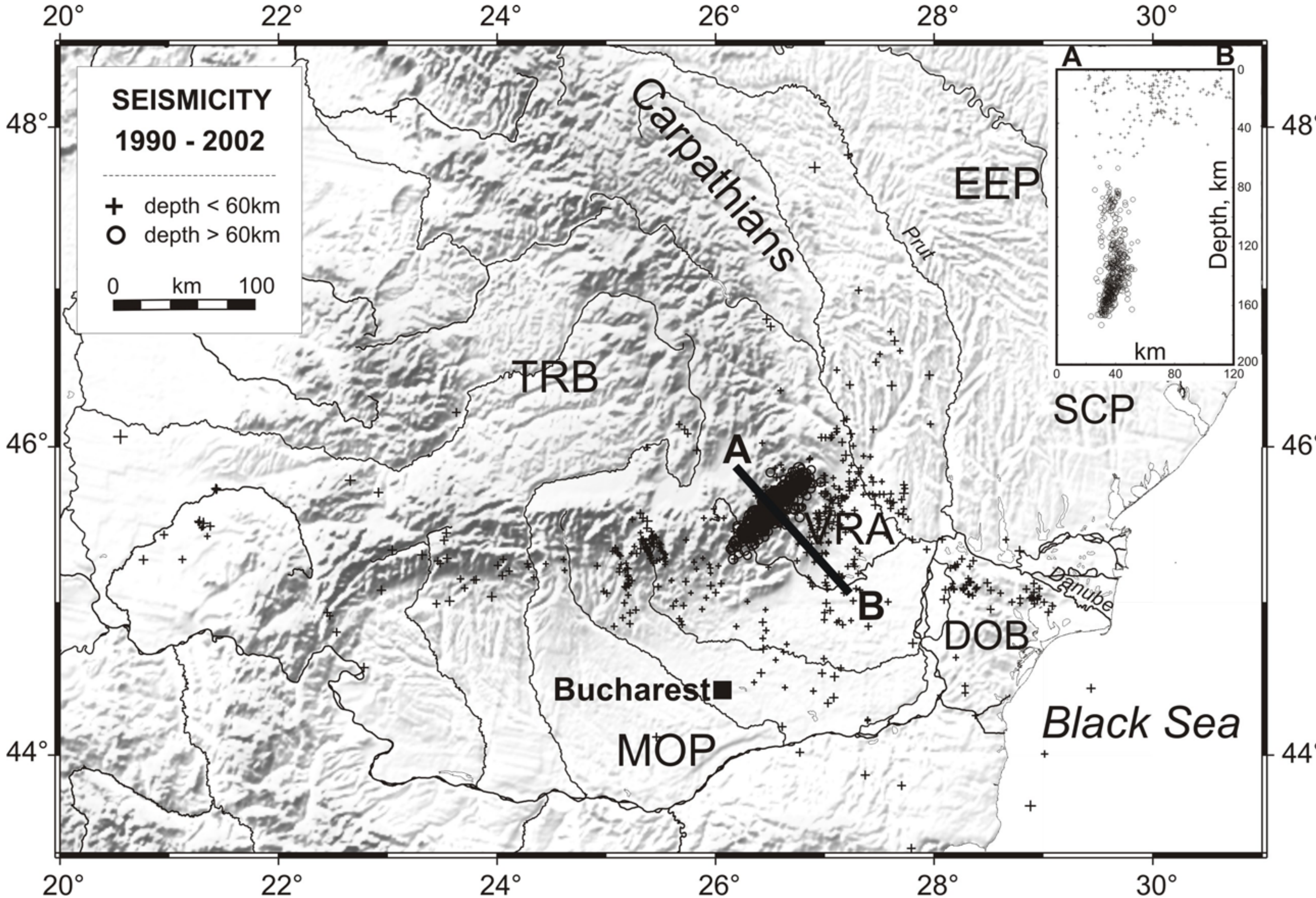
SEISMICITY
1990 - 2002
depth < 60km
depth > 60km
0 km 100
Carpathians
EEP
Prut
TRB
SCP
A
B
VRA
Danube
DOB
Bucharest
MOP
Black Sea
Depth, km
km
20°
22°
24°
26°
28°
30°
44°
46°
48°

Fig. 1

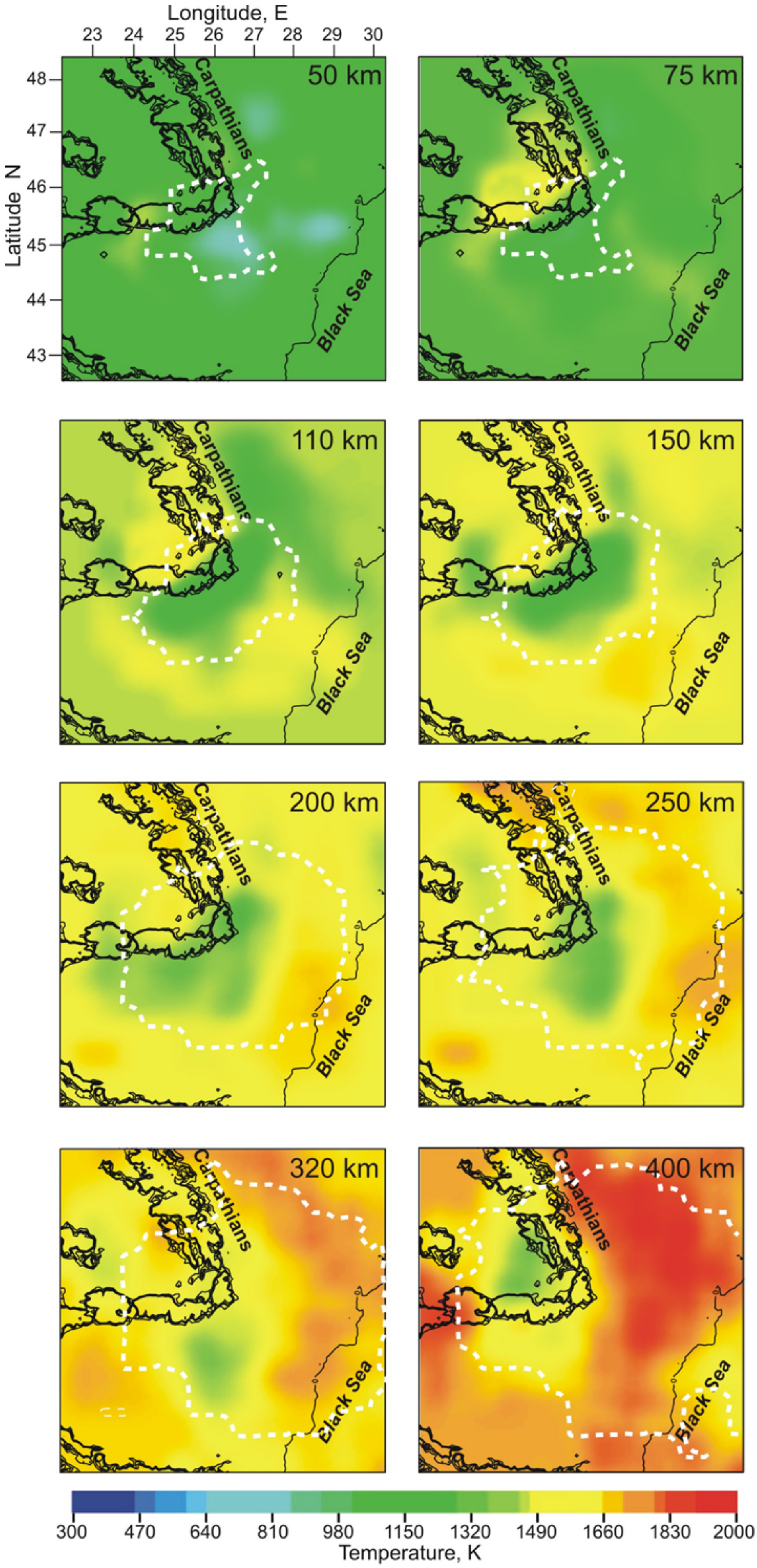

Longitude, E
23
24
25
26
27
28
29
30
Latitude, N
48
47
46
45
44
43
50 km
75 km
110 km
150 km
200 km
250 km
320 km
400 km
Carpathians
Black Sea
300
470
640
810
980
1150
1320
1490
1660
1830
2000
Temperature, K

Fig. 2

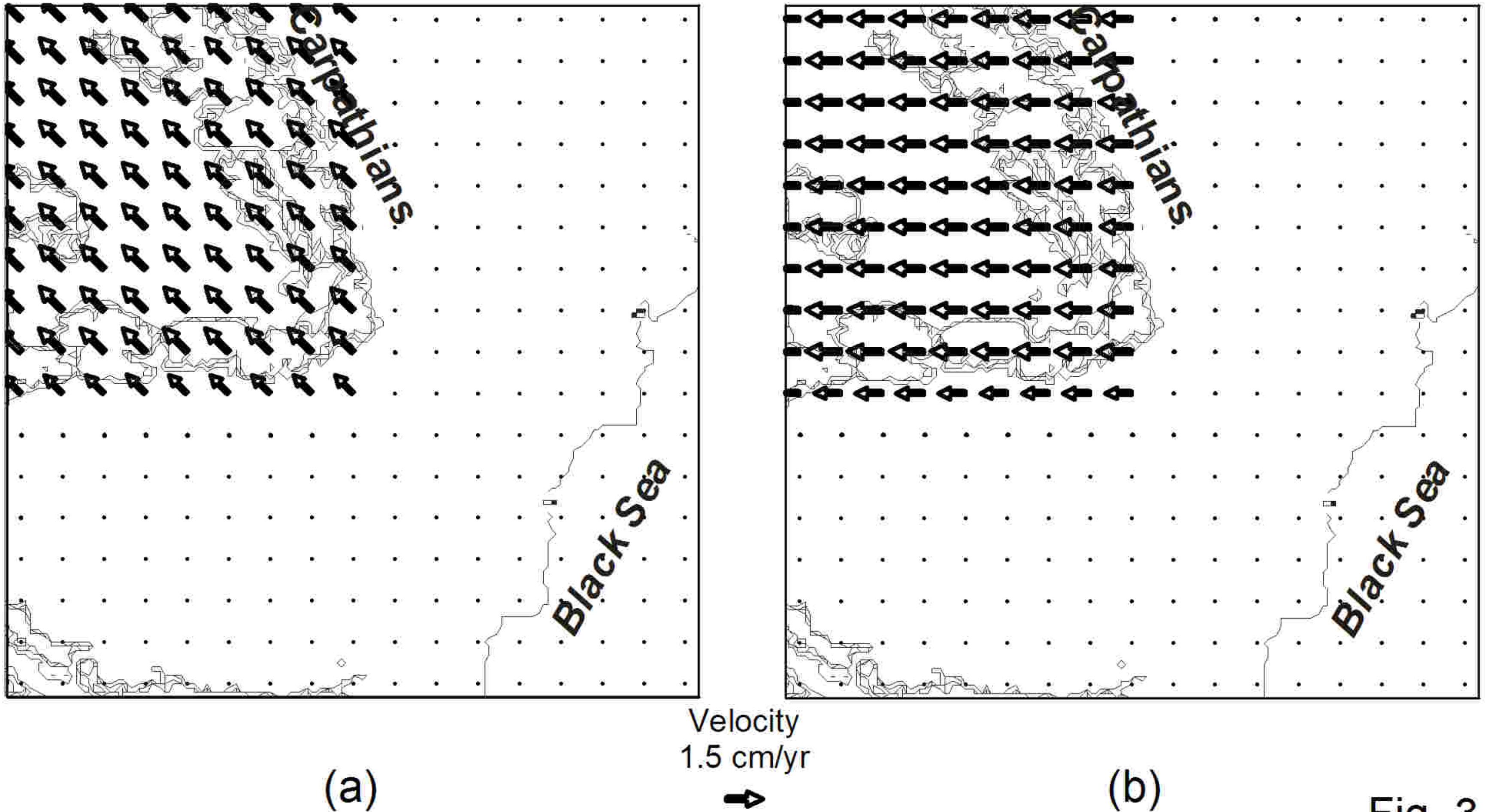

Carpathians
Black Sea
Carpathians
Black Sea
Velocity
1.5 cm/yr
(a)
(b)

Fig. 3

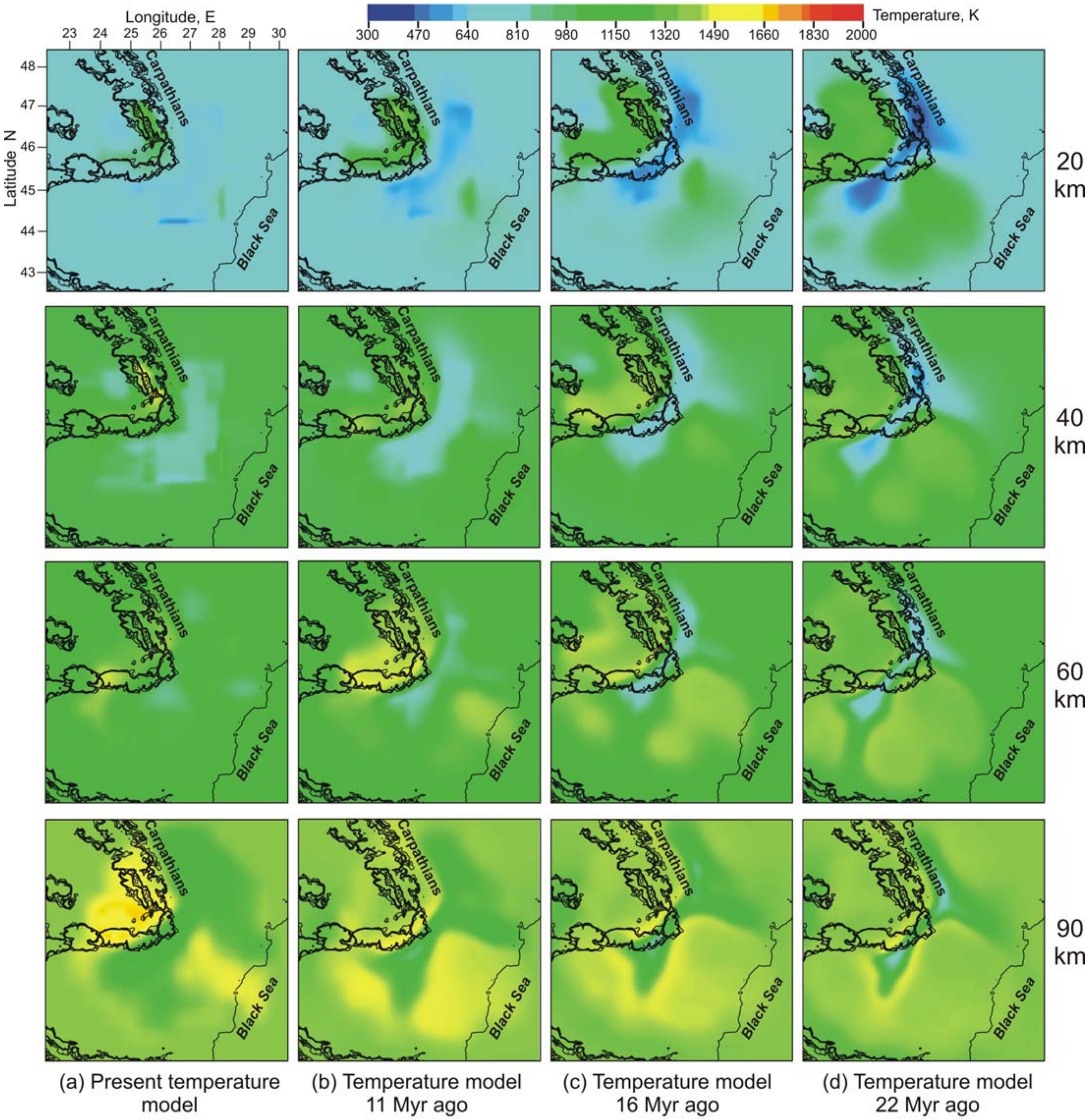

Longitude, E
23 24 25 26 27 28 29 30
Latitude N
48 47 46 45 44 43
300 470 640 810 980 1150 1320 1490 1660 1830 2000
Temperature, K
Carpathians
Black Sea
20 km
40 km
60 km
90 km
(a) Present temperature model
(b) Temperature model 11 Myr ago
(c) Temperature model 16 Myr ago
(d) Temperature model 22 Myr ago

Fig. 4

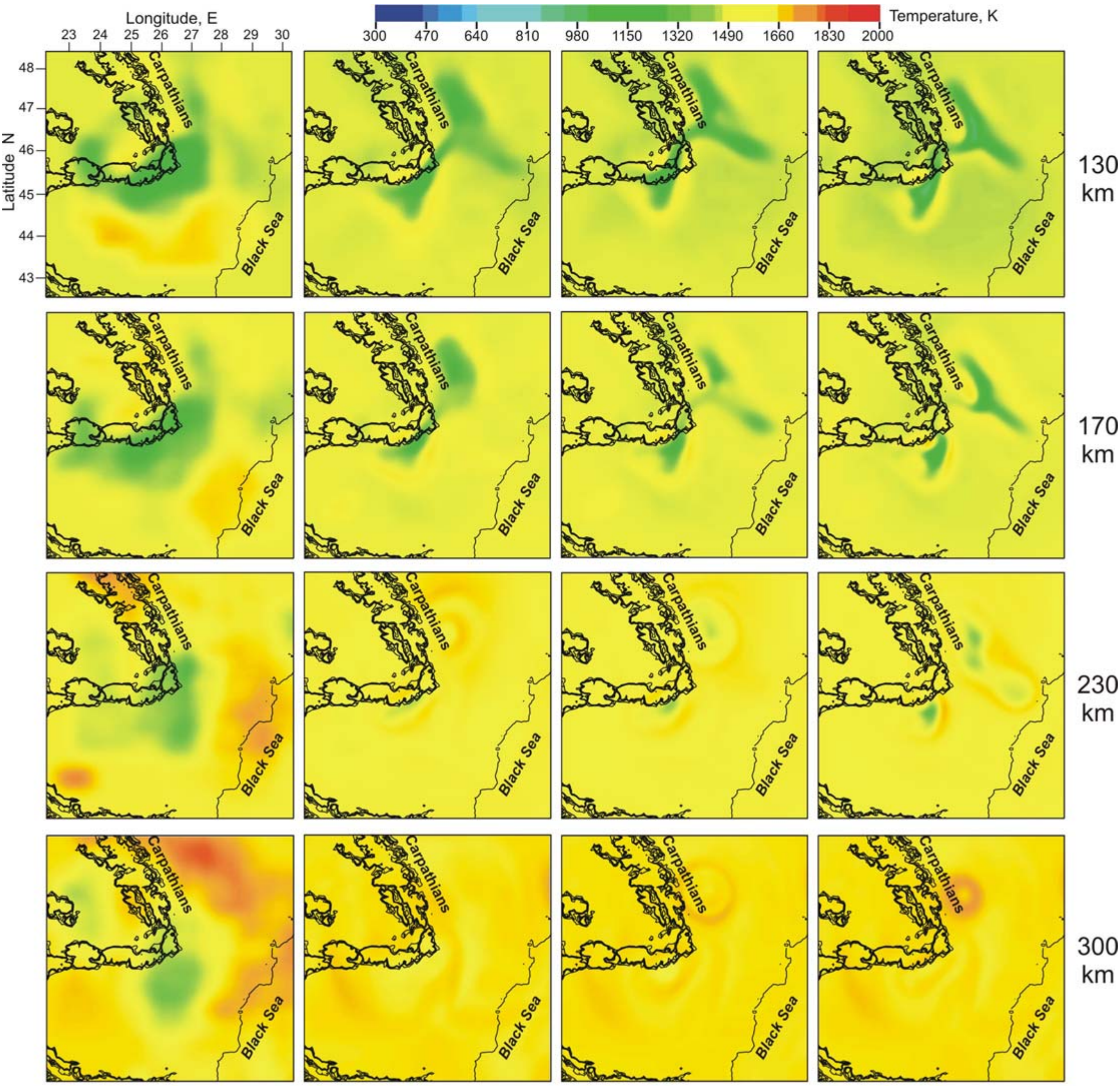

(a) Present temperature model
(b) Temperature model 11 Myr ago
(c) Temperature model 16 Myr ago
(d) Temperature model 22 Myr ago

Fig. 4 (cont.)